Research Square

Preprints are preliminary reports that have not undergone peer review.
They should not be considered conclusive, used to inform clinical practice,
or referenced by the media as validated information.

First-line zanubrutinib-rituximab-methotrexate for newly diagnosed PCNSL (Zana): prospective outcomes and exploratory CSF ctDNA profiling

Wei-Li Zhao

zhao.weili@yahoo.com

Shanghai Institute of Hematology, State Key Laboratory of Medical Genomics, National Research Center for Translational Medicine at Shanghai, Ruijin Hospital affiliated to Shanghai Jiao Tong Universi
https://orcid.org/0000-0002-6834-1616

Li Wang

Shanghai Institute of Hematology, State Key Laboratory of Medical Genomics, National Research Center for Translational Medicine at Shanghai, Ruijin Hospital Affiliated to Shanghai Jiao Tong University
https://orcid.org/0000-0003-2452-0169

Zhizhou Xia

Shanghai Institute of Hematology, State Key Laboratory of Medical Genomics, National Research Center for Translational Medicine at Shanghai, Ruijin Hospital Affiliated to Shanghai Jiao Tong Universi

Mu-Chen Zhang

State Key Laboratory of Medical Genomics, Shanghai Institute of Hematology, Shanghai Rui Jin Hospital, Shanghai Jiao Tong University School of Medicine

Qi Song

Department of Radiology, Ruijin Hospital affiliated to Shanghai Jiao Tong University School of Medicine, Shanghai, China

Qing Shi

State Key Laboratory of Medical Genomics, National Research Center for Translational Medicine, Rui Jin Hospital Affiliated to Shanghai Jiao Tong University School of Medicine, Shanghai, China

Qifan Xu

Shanghai Institute of Hematology, State Key Laboratory of Medical Genomics, National Research Center for Translational Medicine at Shanghai, Ruijin Hospital

Pengpeng Xu

State Key Laboratory of Medical Genomics

Shu Cheng

State Key Laboratory of Medical Genomics

Article

Keywords:

Posted Date: November 24th, 2026

DOI: https://doi.org/10.21203/rs.3.rs-11723847/v1

License: This work is licensed under a Creative Commons Attribution 4.0 International License.
Read Full License

Additional Declarations: There is **NO** conflict of interest to disclose.

Abstract

Primary central nervous system lymphoma (PCNSL) remains an aggressive malignancy with suboptimal long-term control using high-dose methotrexate (HD-MTX)-based therapy. We prospectively evaluated zanubrutinib, rituximab, and HD-MTX (ZRM) and explored cerebrospinal fluid (CSF) circulating tumor DNA (ctDNA) in newly diagnosed, transplantation-ineligible PCNSL. In this investigator-initiated phase II study (NCT05896007), patients received zanubrutinib 160 mg twice daily, rituximab, and HD-MTX for up to six cycles, followed by zanubrutinib maintenance. The primary endpoint was 2-year progression-free survival (PFS); secondary endpoints included response, overall survival (OS), and safety. Exploratory analyses included tumor and CSF genomics and paired profiles. Twenty-nine patients were enrolled (median age 60 years; 72.4% intermediate/high IELSG risk; 58.6% ECOG ≥ 2). The overall response rate was 89.7%, with all responders achieving complete remission. In the per-protocol cohort (n = 25), estimated 2-year PFS and OS were 84.0% and 96.0%, respectively, after median follow-up of 32.5 months. Grade ≥ 3 neutropenia, leukopenia, and thrombocytopenia each occurred in 17.2%; no atrial fibrillation, major bleeding, or invasive fungal infections occurred. Tumor and CSF profiling identified MYD88 and CD79B alterations; higher baseline CSF ctDNA burden and TP53/CXCR4 mutations suggested potential risk associations warranting validation.

Introduction

Primary central nervous system lymphoma (PCNSL) is a rare, aggressive form of extranodal non-Hodgkin lymphoma that arises within the central nervous system (CNS), including the brain, spinal cord, leptomeninges, and eyes[1]. It accounts for approximately 4–6% of primary brain tumors and patients have dismal outcomes. The standard treatment for PCNSL has historically been high-dose methotrexate (HD-MTX)-based chemotherapy, often combined with rituximab and other agents[2].

Recent advances in the molecular biology of PCNSL have highlighted the potential role of Bruton's tyrosine kinase (BTK) inhibitors in the treatment of this disease[3, 4]. BTK is a key mediator in B-cell receptor (BCR) and Toll-like receptor (TLR) signaling pathways[5], which are frequently dysregulated in PCNSL[6]. Zanubrutinib, a second-generation BTK inhibitor, has demonstrated superior selectivity and efficacy compared to first-generation inhibitors, like ibrutinib[7]. Preclinical and early clinical studies have shown that zanubrutinib can effectively penetrate the blood-brain barrier and modulate downstream signaling pathways in PCNSL[8].

Alongside innovations in frontline therapy, efforts to refine consolidation and maintenance strategies are becoming increasingly important. For transplant-eligible individuals, autologous stem-cell transplantation (ASCT) remains a preferred consolidation modality, whereas for older or frail patients, reduced-dose whole-brain radiotherapy (WBRT) may provide disease control but is associated with a risk of neurotoxicity[2, 9].Alternative approaches include maintenance methotrexate (MTX) or less intensive systemic therapies that may be better tolerated in this population, including oral alkylating agents such

as temozolomide and procarbazine, as well as rituximab, lenalidomide, and ibrutinib[10, 11]. Notably, a recent randomized phase II trial comparing myeloablative ASCT with nonmyeloablative consolidation demonstrated that although ASCT yielded superior progression-free survival in the intention-to-treat population, patients who successfully initiated consolidation achieved comparable two-year outcomes regardless of intensity[19]. These findings suggest that less intensive consolidation strategies may provide meaningful disease control for patients unable to tolerate high-dose conditioning. Consistent with this concept, emerging clinical data—including findings from our recent retrospective cohort—suggest that BTK inhibitor–based maintenance therapy may provide a feasible and well-tolerated alternative consolidation strategy, with encouraging durability of remission in patients achieving complete response after induction[12]. Therefore, in this study, we administered maintenance therapy with zanubrutinib to patients who were intolerant to ASCT, aiming to explore a new maintenance strategy for transplantation-ineligible or transplant-unsuitable patients.

Several clinical and biological factors have been associated with outcomes in patients with PCNSL. Age and performance status remain the most consistently validated clinical prognostic factors and form the basis of the two widely used prognostic models, the International Extranodal Lymphoma Study Group (IELSG) score and the Memorial Sloan Kettering Cancer Center (MSKCC) model[13, 14]. Moreover, recurrent genetic alterations involving the NF-κB/B-cell receptor signaling pathway and tumor suppressor pathways have been implicated in disease biology and clinical outcomes. In particular, *TP53* alterations have been associated with inferior survival in subsets of patients with PCNSL[15].

Beyond tumor genomic profiling, liquid biopsy—particularly cerebrospinal fluid (CSF) circulating tumor DNA (ctDNA)—has emerged as a promising tool for monitoring treatment response and detecting molecular alterations in patients with PCNSL[16, 17]. CtDNA analysis in CSF can provide real-time information on tumor burden and genetic mutations, potentially allowing for early detection of treatment resistance and relapse[16]. This study aims to investigate the efficacy and safety of a combination therapy regimen consisting of rituximab, HD-MTX, and zanubrutinib in newly diagnosed PCNSL patients, as well as the correlation between ctDNA changes and treatment outcomes.

Methods

Study design and patients

This single-center, prospective, investigator-initiated trial evaluated the efficacy and safety of the zanubrutinib–rituximab–high-dose methotrexate (ZRM) regimen as first-line therapy for newly diagnosed, transplantation-ineligible PCNSL (ClinicalTrials.gov identifier: NCT05896007). Transplant ineligibility was determined through a multidimensional clinical assessment incorporating age, ECOG performance status, comorbidity burden, cardiac/renal/hepatic function, overall frailty, and the anticipated neurotoxicity of high-dose conditioning[1], together with individual patient preferences and willingness to undergo transplantation.

Eligibility for upfront autologous stem-cell transplantation (ASCT) was assessed at study entry based on performance status, organ function, comorbidity burden, and patient preference, consistent with the multidimensional clinical considerations used in studies of transplant-ineligible lymphoma populations[18]. Four patients initially considered unsuitable for ASCT subsequently proceeded to consolidative ASCT after responding to ZRM induction and discontinued protocol-directed zanubrutinib maintenance. These patients were included in the intention-to-treat response, baseline characteristic, safety, and descriptive treatment-course analyses, but were excluded from the per-protocol PFS and OS analyses. The protocol was approved by the institutional review board in accordance with the Declaration of Helsinki, and all participants provided written informed consent prior to enrollment.

Treatment regimen

Patients received the ZRM regimen, consisting of zanubrutinib 160 mg orally twice daily, rituximab 375 mg/m² on day 1, and HD-MTX 3.5 g/m² on day 2 every 21 days for up to six induction cycles. Leucovorin (folinic acid) rescue was administered according to institutional guidelines to prevent methotrexate-related toxicity. Treatment delay, dose modification, or discontinuation was permitted for toxicity management or physician-assessed clinical need. Patients who achieved complete response after induction continued zanubrutinib maintenance for at least 12 months unless disease progression, unacceptable toxicity, transplantation, withdrawal of consent, or physician decision occurred.

Response assessment

Baseline evaluation included Magnetic Resonance Imaging (MRI) of brain/spine, ophthalmologic examination, and CSF cytology. Radiologic assessments were performed every three cycles using contrast-enhanced brain MRI and positron emission tomography/computed tomography (PET/CT). Treatment responses were evaluated according to the International Primary CNS Lymphoma Collaborative Group (IPCG) criteria by experienced hematologists and radiologists independently. The primary endpoint was 2-year PFS. Secondary endpoints included OS, overall response rate (ORR), complete response (CR) rate, and treatment-related safety. We pre-specified exploratory endpoints to evaluate CSF ctDNA as a biomarker of burden, molecular subtype, and early therapeutic response. ITT included all enrolled patients (n = 29). For patients who completed all six cycles, end-of-induction (EOT) response was defined as the response documented at the post-cycle-6 assessment. For patients who discontinued induction before completing six cycles, the last evaluable response assessment before treatment discontinuation or initiation of subsequent anti-lymphoma therapy was recorded as their final on-induction response. This included one patient who proceeded to consolidative ASCT after achieving CR following cycle 5. Responses obtained after ASCT were not attributed to ZRM induction. Per-protocol survival analyses excluded patients who underwent ASCT after remission (n = 25). Baseline characteristics and safety were summarized in all enrolled patients unless otherwise specified.

Safety monitoring

Adverse events (AEs) were graded according to the National Cancer Institute Common Terminology Criteria for Adverse Events (CTCAE) version 5.0. Laboratory monitoring included complete blood counts, biochemistry panels, and liver and renal function tests before each treatment cycle. Special attention was paid to events previously associated with BTK inhibitors, such as atrial fibrillation, bleeding, and opportunistic fungal infections. Treatment interruptions and dose modifications were recorded. The safety population was included all enrolled patients (n = 29).

Molecular profiling of tumor tissue and CSF ctDNA

Tumor biopsies were obtained at diagnosis when available, and paired cerebrospinal fluid (CSF) samples were collected at baseline and during treatment when available. Tumor DNA was extracted from formalin-fixed paraffin-embedded (FFPE) tissue. Targeted sequencing of lymphoma-related genes was performed using the MultipSeq Custom Panel (Shanghai Rightongene Biotechnology Co., Ltd., China) according to our previously described protocol[19].

CSF circulating tumor DNA (ctDNA) was isolated from CSF supernatant using standard extraction kits. Sequencing libraries were prepared using a hybrid capture–based protocol and subjected to high-depth next-generation sequencing on an Illumina platform, as previously described[20]. Briefly, libraries were constructed and enriched using biotinylated probes targeting lymphoma-related genes and sequenced as paired-end reads.

Tumor specimens and CSF samples were analyzed using a 86-gene lymphoma panel. Sequence alignment, variant calling, and annotation were performed using established bioinformatics pipelines. Variants with an allele frequency ≥ 1% (for CSF ctDNA) and ≥ 5% (for lymphoma tissue) and sequencing coverage ≥ 500× were retained after quality-control filtering. Somatic variants were annotated using COSMIC (v97) and ClinVar.

CtDNA concentration was quantified as haploid genome equivalents per milliliter (hGE/mL). Baseline ctDNA burden was calculated by multiplying the mean variant allele frequency (VAF) across detected mutations by ctDNA concentration and dividing by the weight of a haploid genome (3.3 pg).

Statistical analysis

Categorical variables were summarized as counts and percentages, and continuous variables as medians with ranges. PFS and OS were estimated by Kaplan-Meier methods, with 95% confidence intervals (CIs) derived using Greenwood’s formula. Differences between groups were explored by log-rank tests. Hazard ratios (HRs) were estimated using Cox proportional hazards models. Given the limited number of events, penalized likelihood estimation using the Firth correction was applied when

appropriate to reduce small-sample bias. Statistical significance was defined as a two-sided $P < 0.05$. Analyses were performed using R version 4.2.

Results

Patient enrollment and baseline characteristics

Between July 2023 and July 2025, a total of 29 patients with newly diagnosed PCNSL were prospectively enrolled in this trial (NCT05896007) and initiated ZRM induction therapy. Baseline demographics and disease characteristics are summarized in Table 1. The median age was 60 years (range, 30–75), and 17 patients (58.6%) were male. Seventeen patients (58.6%) had an Eastern Cooperative Oncology Group (ECOG) performance status of ≥ 2.

Table 1
Baseline clinical characteristics of the ZANA PCNSL cohort

Characteristic	Overall cohort
	N = 29
Age, years	
Median	60 (30, 75)
≥ 60	15 (51.7%)
Sex, n (%)	
Male	17 (58.6%)
Female	12 (41.4%)
ECOG performance status, n (%)	
0–1	12 (41.4%)
≥ 2	17 (58.6%)
Elevated LDH, U/L	
Yes	5 (17.2%)
No	24 (82.8%)
IELSG risk, n (%)	
Low	8 (27.6%)
Intermediate	15 (51.7%)
High	6 (20.7%)
MSKCC prognostic class, n (%)	
Class 1 (low)	5 (17.2%)
Class 2 (intermediate)	12 (41.4%)
Class 3 (high)	12 (41.4%)
COO subtype, n (%)	
GCB	5 (17.2%)
non-GCB	22 (75.9%)
*Unknown**	2 (6.9%)

* Clonal B-cell infiltration was confirmed by flow cytometry of the aqueous humor or cerebrospinal fluid; however, the cellular origin could not be determined.

Characteristic	Overall cohort
	N = 29
Age, years	
DEL status, n (%)	
DE	10 (34.5%)
non-DE	15 (51.7%)
Unknown	4 (13.8%)
Brain parenchymal involvement, n (%)	27 (93.1%)
Meningeal/CSF involvement, n (%)	3 (10.3%)
Eye involvement, n (%)	1 (3.4%)
Previous surgery/biopsy, n (%)	
Craniotomy/resection	17 (58.6%)
Biopsy	12 (41.4%)
* Clonal B-cell infiltration was confirmed by flow cytometry of the aqueous humor or cerebrospinal fluid; however, the cellular origin could not be determined.	

Brain parenchymal involvement was documented in 27 patients (93.1%), meningeal or CSF involvement in 3 (10.3%), and ocular involvement in 1 (3.4%). Intracranial lesions most frequently involved the frontal lobes (n = 9, 31.0%), basal ganglia (n = 7, 24.1%), parietal lobes (n = 5, 17.2%), cerebellum (n = 4, 13.8%), and occipital lobes (n = 3, 10.3%). Other locations included the corpus callosum (n = 2, 6.9%), brainstem or midbrain (n = 2, 6.9%), and less frequently the temporal lobe, thalamus, cerebellopontine angle, cerebellar peduncle, and suprasellar cistern (n = 1 each, 3.4%).

Elevated serum LDH was observed in 5 patients (17.2%). By IELSG criteria, 21 patients (72.4%) were classified as intermediate-to-high risk. According to the MSKCC scoring system, 24 patients (82.8%) fell into the intermediate- or high-risk categories. Four young patients (13.8%) proceeded to ASCT after achieving remission and were excluded from per-protocol survival analysis but included in baseline and safety evaluations. Among the remaining 4 younger patients (aged 30–55 years) who did not undergo ASCT, two declined transplantation, one had severe renal impairment (stage 4), and one had poor baseline performance status (ECOG 4) with primary refractory disease and subsequently died after cycle 6 of induction.

Clinical Efficacy

All 29 patients initiated study treatment, with a median of six cycles administered (range, 3–6). Twenty-five patients (86.2%) completed all six planned cycles. Among the four patients who discontinued

induction early, three had progressive disease (PD) and subsequently received alternative anti-lymphoma therapy, whereas one achieved CR after five cycles and proceeded to consolidative ASCT. Treatment exposure and individual response courses are illustrated in the swimmer plot (Fig. 2C).

At the end of induction, the ITT objective response rate (ORR) was 89.7% (26/29; 95% CI, 72.7–97.8), with all responders achieving CR (CRR = 89.7%). Three patients (10.3%) did not achieve complete response, all of whom experienced progressive disease.

For survival analyses, four patients who underwent ASCT after remission were excluded from the per-protocol cohort, leaving 25 patients for PFS and OS evaluation. After a median follow-up of 32.5 months, the estimated 2-year PFS was 84.0% (95% CI, 70.8–99.7) and the 2-year OS was 96.0% (95% CI, 88.6–100) (Fig. 2A-B). At data cutoff, five progression events and two deaths had occurred. Because of the limited number of events, multivariable Cox modeling was not feasible. Exploratory results of baseline clinical and molecular factors are summarized in Supplementary Table 1, with no significant clinicopathological factors identified as being associated with patient outcomes.

Safety

The ZRM regime treatment was well tolerated. Treatment-emergent adverse events (AEs) are listed in Table 2. The most common grade ≥ 3 hematologic toxicities were neutropenia, leukopenia, and thrombocytopenia (each 17.2%). Grade 3 liver transaminase elevations occurred in one patient (3.4%). Importantly, no atrial fibrillation, major bleeding, or invasive fungal infections were observed–adverse events that have limited the application of first-generation BTK inhibitors in PCNSL. No treatment-related deaths occurred.

Tumor genomic alterations

Targeted sequencing of available tumor tissue was performed in 20 of 29 patients. The mutational landscape was dominated by recurrent alterations in canonical PCNSL drivers. The most frequently mutated genes were *MYD88*, *CD79B*, *PIM1*, and *BTG2*, with mutation frequencies of 94%, 89%, 72%, and 44%, respectively (Fig. 3A). Indeed, subtype classification using both LymphPlex and LymphGen algorithms (Supplementary Fig. 1) placed the majority of tumors in the MCD category, in line with previous genomic studies of PCNSL[21].

We further compared tumor mutation profiles between patients with and without PD. TP53 mutations were more frequent in patients with progression than in those without progression (2/4 [50.0%] vs. 0/13 [0%]; nominal Fisher's exact P = 0.044; Fig. 3B).To further prioritize tumor-derived candidate alterations, we performed exploratory univariate analyses for PFS in the tumor-tissue cohort. Mutations in *TP53, ID3, STAT6 and STAT3* were associated with inferior PFS, while *CXCR4* showed adverse trends with wide confidence intervals (Fig. 3C).

Baseline CSF ctDNA burden and genomic profiling identify molecular correlates of disease progression

Baseline CSF ctDNA sequencing was successfully performed in 21 of 29 patients. After quality-control filtering, 18 patients with detectable somatic mutations and were included in the mutational landscape analysis. The mutational profile was characterized by recurrent alterations in canonical PCNSL-associated genes, with *MYD88* and *CD79B*, representing the most frequently mutated genes (Fig. 4A). We next compared baseline mutational profiles between patients who subsequently experienced disease progression and those who remained progression-free. Exploratory mutation-frequency analyses identified enrichment of *CD79B*, *CXCR4* and *TBL1XR1* mutations among patients who progressed, with additional candidate progression-associated alterations involving *BTG2* and *TP53* (Fig. 4B). Consistent with these findings, exploratory univariable Cox analyses revealed associations between *CD79B*, *CXCR4*, *TBL1XR1* and *TP53* mutations and inferior outcomes(Fig. 4C).

To evaluate the ability of CSF ctDNA sequencing to capture the genomic landscape of PCNSL, we compared mutation profiles in paired diagnostic tumor tissue and baseline CSF samples. Among 13 patients with paired specimens, 11 had evaluable mutation profiles after quality-control filtering and were included in the concordance analysis. Across the 86 genes in the panel, 35 of 104 tumor-reported patient–gene observations (33.7%) were detected in matched CSF samples. The median patient-level co-detection fraction was 25.0% (range, 0–83.3%), indicating substantial interpatient variability. In addition, 23 patient–gene observations were reported exclusively in CSF, suggesting that CSF sequencing may provide genomic information complementary to tumor tissue profiling (Fig. 5A). Importantly, the proportion of tumor-reported genes also detected in CSF was positively correlated with baseline CSF ctDNA abundance (Spearman $\rho = 0.783$, permutation $P = 0.0065$; Holm-adjusted $P = 0.0326$). This finding suggests that higher CSF ctDNA abundance is associated with more extensive recovery of tumor-reported genomic alterations in CSF (Fig. 5B). Paired oncoplot analysis demonstrated that CSF ctDNA captured canonical PCNSL-associated alterations, including *MYD88* and *CD79B*, in multiple patients. Notably, *CD79B* alterations were co-detected in tumor tissue and CSF in six patients (54.5%) and were highlighted in the paired analysis (Fig. 5A–B). These findings support the utility of CSF ctDNA as a complementary approach to tumor tissue sequencing while highlighting the potential influence of tumor burden on mutation detection.

We next investigated the prognostic significance of quantitative baseline CSF ctDNA burden. Quantitative measurements were available for 17 patients in the intention-to-treat population, including 16 who did not subsequently undergo ASCT. In this exploratory non-ASCT subset, patients with disease progression had higher baseline CSF ctDNA levels than those without progression (Wilcoxon $P = 0.014$; Fig. 6A).

Using a fixed exploratory cutoff of 2.695 log10 hGE/mL, patients were classified into high and low baseline ctDNA groups. Higher baseline ctDNA burden was associated with shorter PFS in this subset (log-rank $P = 0.019$; Fig. 6B).

We further examined ctDNA dynamics in the three patients who subsequently experienced disease progression. One patient showed minimal ctDNA reduction, whereas the other two exhibited substantial

early declines despite later disease progression. Notably, the latter two patients harbored high-risk genomic alterations involving *TP53* or *CXCR4* (Figure 6C). These observations suggest that baseline CSF ctDNA burden may help predict treatment response, whereas longitudinal ctDNA monitoring may provide complementary value in detecting emerging treatment resistance, particularly when interpreted in the context of underlying molecular risk.

Discussion

This prospective, registered clinical trial demonstrates that the combination of zanubrutinib, rituximab, and high-dose methotrexate followed by zanubrutinib maintenance (ZRM) achieves deep and durable remissions in newly diagnosed PCNSL patients considered unsuitable for upfront ASCT. The cohort was predominantly composed of individuals with intermediate- to high-risk disease (IELSG intermediate/high-risk 72.4%, ECOG ≥ 2 in 58.6%). Among 29 patients, the ORR was 89.7%, with all responders achieving CR. After a median follow-up of 32.5 months, the 2-year PFS and OS were 84.0% and 96.0%, respectively. The regimen was generally well tolerated, with manageable hematologic toxicity and no observed atrial fibrillation, major bleeding, invasive fungal infection, or treatment-related death. Although the single-arm design precludes direct comparison with historical regimens, these outcomes support further evaluation of ZRM as a frontline strategy for transplantation-unsuitable PCNSL.

Historically, frontline HD-MTX-based chemotherapy has produced CR rates of only 40–60% and 2-year PFS of 30–50%, with median OS rarely exceeding 40 months[22, 23]. By comparison, the addition of zanubrutinib clearly improves long-term disease control, with 2-year PFS and OS outcomes surpassing historical benchmarks. The frequent *MYD88* L265P and *CD79B* Y196 alterations in PCNSL provide a biological rationale for targeting the TLR/BCR–NF-κB signaling axis through BTK inhibition, while the cerebrospinal fluid penetration of zanubrutinib further supports its therapeutic potential in this CNS-restricted disease[21, 24–26].

Consistent with our findings, the multicenter phase II MIT trial (HD-MTX + ibrutinib + temozolomide) achieved an ORR of 93.9% but only a 2-year PFS of 57.6% and was complicated by opportunistic fungal infections[27]. The R-MO regimen (rituximab, HD-MTX, orelabrutinib) achieved an ORR of approximately 90% and 1-year PFS of around 80%[28]. Together with our results, these data suggest that next-generation BTK inhibitors achieve comparable or superior efficacy with improved safety in the CNS setting.

Despite of the favorable efficacy, treatment was well tolerated. Grade ≥ 3 hematologic toxicities occurred in approximately 17% of patients, and non-hematologic events were mainly grade 1–2, including mild transaminase elevation and mucositis. No atrial fibrillation, major bleeding, or invasive fungal infections were observed—contrasting with ibrutinib-associated infectious morbidity in prior studies[29]. The favorable safety profile likely reflects zanubrutinib's high kinase selectivity and sustained CNS exposure without excess off-target inhibition.

Genomic profiling revealed frequent alterations involving *MYD88* and *CD79B*, consistent with the established molecular landscape of PCNSL. Exploratory analyses of tumor tissue identified nominal associations of *TP53*, *ID3*, *STAT6*, and *STAT3* alterations with shorter PFS. *TP53* plays a central role in DNA-damage responses, cell-cycle regulation, and apoptosis. Loss of p53 function may impair these protective mechanisms and contribute to reduced sensitivity to cytotoxic therapy[30]. Importantly, a recent genomic study of newly diagnosed PCNSL also identified *TP53* mutations as being associated with disease progression and shorter PFS[15]. Of particular interest, *CD79B* alterations were detected in all three patients with recorded progression in the non-ASCT CSF cohort.

The use of ctDNA analysis in CSF has provided valuable insights into the genetic landscape of PCNSL and its correlation with treatment response[16, 20, 27, 31, 32]. Baseline CSF ctDNA burden was significantly higher in patients who subsequently progressed. Previous studies have reported that ctDNA levels correlate with tumor burden and the number of genomic alterations, suggesting that ctDNA burden may reflect the underlying tumor burden and biological aggressiveness[33]. Canonical drivers (*MYD88* and *CD79B*) were consistently detected, validating CSF as a reliable surrogate of the PCNSL genomic backbone[17, 34]. *TP53* mutations, which were associated with disease progression in tumor tissue, also showed trends toward inferior PFS when detected in CSF ctDNA. These findings suggest that CSF ctDNA can identify progression-associated molecular signals, but they require validation in larger cohorts with adequate event numbers and prespecified multiplicity control. The *CXCL12–CXCR4* signaling axis has been implicated in the perivascular localization of malignant B cells in PCNSL, providing a potential biological context for the exploratory association of *CXCR4* alterations with clinical outcomes[35]. *CXCR4* mutations are enriched in PCNSL compared with systemic DLBCL, potentially contributing to BTK inhibitor resistance[36–38]. *TBL1XR1*, recurrently altered in PCNSL, drives *NF-κB* and *Wnt* pathway dysregulation[39–41]. Taken together, these findings reinforce the importance of *CXCR4* and *TBL1XR1* as molecular determinants of PCNSL outcome, and suggest that targeting these pathways may improve therapeutic efficacy in high-risk patients.

The incomplete concordance between tumor tissue and CSF ctDNA mutation profiles may reflect not only the spatial heterogeneity previously documented in PCNSL but also differences in mutation detection sensitivity between the two approaches[34]. In addition, ctDNA detection may be influenced by several factors, including tumor shedding into the CSF, lesion proximity to CSF spaces, sampling time, and variant-level detection thresholds[32]. These data support CSF ctDNA as a complementary molecular profiling source, particularly when tumor tissue is limited or unavailable, but not as a fully interchangeable replacement for tissue-based profiling.

Several limitations should be acknowledged. This was a single-center study with a modest sample size, limiting power for subgroup analyses and precluding robust multivariable modeling. Larger, prospective studies are warranted to validate these findings.

Despite these limitations, this study provides novel prospective evidence for the efficacy and tolerability of zanubrutinib-based induction and maintenance in newly diagnosed PCNSL patients considered unsuitable for upfront ASCT. Our study also found that baseline CSF ctDNA burden was prognostic, while mutations in *CXCR4*, *CD79B*, *TBL1XR1*, and *TP53*were enriched in patients who experienced disease progression following ZRM treatment, suggesting that these alterations may be associated with inferior outcomes with this regimen. Larger prospective studies are warranted to validate these findings.

Declarations

Competing interests

The authors declare no competing interests.

Funding

This study was supported, in part, by research funding from Noncommunicable Chronic Diseases-National Science and Technology Major Project (2026ZD0553900, 2023ZD0500700, 2023ZD0511200), National Natural Science Foundation of China (82570246, 82530008, 82130004), Shanghai Lymphoma Clinical Cohort of Shanghai Hospital Development Center (SHDC2025CCS008), International Joint Laboratory Construction Program of the Science and Technology Commission of Shanghai Municipality (25TS1404000, 25410750300), Shanghai Clinical Research Center for Cell Therapy (23J41900100), Collaborative Innovation Center of Systems Biomedicine, and Clinical Research Project of Shanghai Municipal Health Commission (20244Y0107).

Author Contributions

Zhi-Zhou Xia, Mu-Cheng Zhang, Qi Song, and Qing Shi contributed equally to this work. Zhi-Zhou Xia led the data collection, data analysis, and manuscript drafting. Mu-Cheng Zhang, and Qing Shi contributed to patient enrollment, data collection. Qi Song was responsible for radiological assessment and imaging evaluation. Qi-Fan Xu contributed to sample processing, Shu Cheng and Peng-Peng Xu participated in data collection and patient management. Wei-Li Zhao and Li Wang designed, supervised the study and contributed to data interpretation and manuscript revision.

References

1. Ferreri AJM, Calimeri T, Cwynarski K, Dietrich J, Grommes C, Hoang-Xuan K *et al.*Primary central nervous system lymphoma. *Nat Rev Dis Primers* 2023; 9(1): 29. e-pub ahead of print 20230615; doi: 10.1038/s41572-023-00439-0

2. Schaff LR, Grommes C. Primary central nervous system lymphoma. *Blood* 2022; 140(9): 971–979. doi: 10.1182/blood.2020008377
3. Wang L, Guo M, Hou S. Advances in primary large B-cell lymphoma of immune-privileged sites. *Front Immunol* 2025; 16: 1533444. e-pub ahead of print 20250226; doi: 10.3389/fimmu.2025.1533444
4. Wei R, Yang S. Advances in first-line treatment for primary central nervous system lymphoma: highlights from the 2025 ASH annual meeting. *J Hematol Oncol* 2026; 19(1). e-pub ahead of print 20260409; doi: 10.1186/s13045-026-01786-7
5. Mandato E, Yan Q, Ouyang J, Paczkowska J, Qin Y, Hao Y *et al.* MYD88L265P augments proximal B-cell receptor signaling in large B-cell lymphomas via an interaction with DOCK8. *Blood* 2023; 142(14): 1219–1232. doi: 10.1182/blood.2023019865
6. Jiang H, Nong L. The Landscape of Primary Central Nervous System Lymphoma (PCNSL): Clinicopathologic and Genomic Characteristics and Therapeutic Perspectives. *Cancers (Basel)* 2025; 17(17). e-pub ahead of print 20250904; doi: 10.3390/cancers17172909
7. Yu H, Kong H, Li C, Dong X, Wu Y, Zhuang Y *et al.* Bruton's tyrosine kinase inhibitors in primary central nervous system lymphoma-evaluation of anti-tumor efficacy and brain distribution. *Transl Cancer Res* 2021; 10(5): 1975–1983. doi: 10.21037/tcr-21-50
8. Yadav BS. High-dose methotrexate and zanubrutinib combination therapy for primary central nervous system lymphoma. *World J Clin Oncol* 2024; 15(3): 371–374. doi: 10.5306/wjco.v15.i3.371
9. Li M, Peng R, Bao F, Jing H, Wang H. Role of Radiotherapy in PCNSL within the Current Therapeutic Landscape: a Comprehensive Review. *Curr Treat Options Oncol* 2025; 26(6): 486–499. e-pub ahead of print 20250508; doi: 10.1007/s11864-025-01327-3
10. Chen T, Liu Y, Wang Y, Chang Q, Wu J, Wang Z *et al.*Evidence-based expert consensus on the management of primary central nervous system lymphoma in China. *J Hematol Oncol* 2022; 15(1): 136. e-pub ahead of print 20220929; doi: 10.1186/s13045-022-01356-7
11. Batchelor TT, Giri S, Ruppert AS, Geyer SM, Smith SE, Mohile N *et al.* Myeloablative vs nonmyeloablative consolidation for primary central nervous system lymphoma: results of Alliance 51101. *Blood Adv* 2024; 8(12): 3189–3199. doi: 10.1182/bloodadvances.2023011657
12. Xu QF, Shen R, Shen YG, Cao YW, Qian Y, Xu PP *et al.* [Clinicopathologic characteristics and survival analysis of primary large B-cell lymphoma of the central nervous system]. *Zhonghua Xue Ye Xue Za Zhi* 2024; 45(5): 481–487. doi: 10.3760/cma.j.cn121090-20231126-00278
13. Ferreri AJ, Blay JY, Reni M, Pasini F, Spina M, Ambrosetti A *et al.* Prognostic scoring system for primary CNS lymphomas: the International Extranodal Lymphoma Study Group experience. *J Clin Oncol* 2003; 21(2): 266–272. doi: 10.1200/JCO.2003.09.139
14. Abrey LE, Ben-Porat L, Panageas KS, Yahalom J, Berkey B, Curran W *et al.*Primary central nervous system lymphoma: the Memorial Sloan-Kettering Cancer Center prognostic model. *J Clin Oncol* 2006; 24(36): 5711–5715. e-pub ahead of print 20061120; doi: 10.1200/JCO.2006.08.2941
15. Geng H, Mo S, Chen L, Ballapuram A, Tsang M, Lu M *et al.* Identification of genomic biomarkers of disease progression and survival in primary CNS lymphoma. *Blood Adv* 2025; 9(5): 1117–1131. doi:

10.1182/bloodadvances.2024014460

16. Zheng MM, Zhou Q, Chen HJ, Jiang BY, Tang LB, Jie GL *et al.*Cerebrospinal fluid circulating tumor DNA profiling for risk stratification and matched treatment of central nervous system metastases. *Nat Med* 2025; 31(5): 1547–1556. e-pub ahead of print 20250227; doi: 10.1038/s41591-025-03538-5
17. Gupta M, Burns EJ, Georgantas NZ, Thierauf J, Nayyar N, Gordon A *et al.* A rapid genotyping panel for detection of primary central nervous system lymphoma. *Blood* 2021; 138(5): 382–386. doi: 10.1182/blood.2020010137
18. Abramson JS, Ku M, Hertzberg M, Huang HQ, Fox CP, Zhang H *et al.* Glofitamab plus gemcitabine and oxaliplatin (GemOx) versus rituximab-GemOx for relapsed or refractory diffuse large B-cell lymphoma (STARGLO): a global phase 3, randomised, open-label trial. *Lancet (London, England)* 2024; 404(10466): 1940–1954. doi: 10.1016/S0140-6736(24)01774-4
19. Shen R, Fu D, Dong L, Zhang MC, Shi Q, Shi ZY *et al.*Simplified algorithm for genetic subtyping in diffuse large B-cell lymphoma. *Signal Transduct Target Ther* 2023; 8(1): 145. e-pub ahead of print 20230410; doi: 10.1038/s41392-023-01358-y
20. Liang JH, Wu YF, Shen HR, Li Y, Liang JH, Gao R *et al.*Clinical implications of CSF-ctDNA positivity in newly diagnosed diffuse large B cell lymphoma. *Leukemia* 2024; 38(7): 1541–1552. e-pub ahead of print 20240515; doi: 10.1038/s41375-024-02279-7
21. Hernandez-Verdin I, Kirasic E, Wienand K, Mokhtari K, Eimer S, Loiseau H *et al.*Molecular and clinical diversity in primary central nervous system lymphoma. *Ann Oncol* 2023; 34(2): 186–199. e-pub ahead of print 20221117; doi: 10.1016/j.annonc.2022.11.002
22. Ferreri AJM, Illerhaus G, Doorduijn JK, Auer DP, Bromberg JEC, Calimeri T *et al.*Primary central nervous system lymphomas: EHA-ESMO Clinical Practice Guideline for diagnosis, treatment and follow-up. *Ann Oncol* 2024. e-pub ahead of print 20240514; doi: 10.1016/j.annonc.2023.11.010
23. Houillier C, Taillandier L, Dureau S, Lamy T, Laadhari M, Chinot O *et al.* Radiotherapy or Autologous Stem-Cell Transplantation for Primary CNS Lymphoma in Patients 60 Years of Age and Younger: Results of the Intergroup ANOCEF-GOELAMS Randomized Phase II PRECIS Study. *J Clin Oncol* 2019; 37(10): 823–833. e-pub ahead of print 20190220; doi: 10.1200/JCO.18.00306
24. Fukumura K, Kawazu M, Kojima S, Ueno T, Sai E, Soda M *et al.*Genomic characterization of primary central nervous system lymphoma. *Acta Neuropathol* 2016; 131(6): 865–875. e-pub ahead of print 20160112; doi: 10.1007/s00401-016-1536-2
25. Roschewski M, Hodson DJ. Diffuse large B-cell lymphoma involving the central nervous system: biologic rationale for targeted therapy. *Haematologica* 2024; 109(2): 388–400. e-pub ahead of print 20240201; doi: 10.3324/haematol.2021.278613
26. Zhang Y, Li Y, Zhuang Z, Wang W, Wei C, Zhao D *et al.*Preliminary Evaluation of Zanubrutinib-Containing Regimens in DLBCL and the Cerebrospinal Fluid Distribution of Zanubrutinib: A 13-Case Series. *Frontiers in oncology* 2021; 11: 760405. e-pub ahead of print 20211224; doi: 10.3389/fonc.2021.760405

27. Gao Y, Ping L, Shan C, Huang H, Li Z, Zhou H *et al.* High-Dose Methotrexate, Ibrutinib, and Temozolomide in the Treatment of Newly Diagnosed Primary CNS Lymphoma: A Multicenter, Prospective Phase II Study. *Blood Cancer Discov* 2025; 6(3): 191–202. doi: 10.1158/2643-3230.BCD-24-0156
28. Sheng L, Liu H, Zhang X, Ding K, Ma J, Peng H *et al.*Prospective phase II trial of first-line rituximab, methotrexate, and orelabrutinib (R-MO) in primary central nervous system lymphoma. *Blood Cancer J* 2025; 15(1): 81. e-pub ahead of print 20250429; doi: 10.1038/s41408-025-01278-w
29. Lionakis MS, Dunleavy K, Roschewski M, Widemann BC, Butman JA, Schmitz R *et al.*Inhibition of B Cell Receptor Signaling by Ibrutinib in Primary CNS Lymphoma. *Cancer cell* 2017; 31(6): 833–843 e835. e-pub ahead of print 20170525; doi: 10.1016/j.ccell.2017.04.012
30. Kastenhuber ER, Lowe SW. Putting p53 in Context. *Cell* 2017; 170(6): 1062–1078. doi: 10.1016/j.cell.2017.08.028
31. Song GY, Park JH, Kang SR, Han SJ, Jung Y, Son M *et al.*Clinical Implication of Sequential Circulating Tumor DNA Assessments for the Treatment of Diffuse Large B-Cell Lymphoma. *Cancers (Basel)* 2025; 17(11). e-pub ahead of print 20250522; doi: 10.3390/cancers17111734
32. Mutter JA, Alig SK, Esfahani MS, Lauer EM, Mitschke J, Kurtz DM *et al.*Circulating Tumor DNA Profiling for Detection, Risk Stratification, and Classification of Brain Lymphomas. *J Clin Oncol* 2023; 41(9): 1684–1694. e-pub ahead of print 20221221; doi: 10.1200/JCO.22.00826
33. Shi Q, Zhang M, He Y, Lin R, Cai M, Zhong H *et al.*Baseline tumor-informed circulating tumor DNA concentration predicts early chemoimmunotherapy failure in diffuse large B-cell lymphoma. *Cancer Lett* 2026; 640: 218249. e-pub ahead of print 20260108; doi: 10.1016/j.canlet.2026.218249
34. Heming M, Haessner S, Wolbert J, Lu IN, Li X, Brokinkel B *et al.*Intratumor heterogeneity and T cell exhaustion in primary CNS lymphoma. *Genome Med* 2022; 14(1): 109. e-pub ahead of print 20220924; doi: 10.1186/s13073-022-01110-1
35. Venetz D, Ponzoni M, Schiraldi M, Ferreri AJ, Bertoni F, Doglioni C *et al.* Perivascular expression of CXCL9 and CXCL12 in primary central nervous system lymphoma: T-cell infiltration and positioning of malignant B cells. *Int J Cancer* 2010; 127(10): 2300–2312. doi: 10.1002/ijc.25236
36. Zhu YX, Wong JC, Hilal T, Maguire A, Ocal J, Zellner K *et al.*Primary Central Nervous System Lymphoma Tumor Biopsies Show Heterogeneity in Gene Expression Profiles and Genetic Subtypes. *medRxiv* 2025. e-pub ahead of print 20250414; doi: 10.1101/2024.11.11.24316310
37. Babst N, Isbell LK, Rommel F, Tura A, Ranjbar M, Grisanti S *et al.*CXCR4, CXCR5 and CD44 May Be Involved in Homing of Lymphoma Cells into the Eye in a Patient Derived Xenograft Homing Mouse Model for Primary Vitreoretinal Lymphoma. *Int J Mol Sci* 2022; 23(19). e-pub ahead of print 20221004; doi: 10.3390/ijms231911757
38. He M, Zhang W, Wang J, Gao L, Jiao L, Wang L *et al.* Aggregative Perivascular Tumor Cell Growth Pattern of Primary Central Nervous System Lymphomas Is Associated with Hypoxia-Related Endoplasmic Reticulum Stress. *J Cancer* 2021; 12(13): 3841–3852. e-pub ahead of print 20210505; doi: 10.7150/jca.54952

39. Grommes C, Nandakumar S, Schaff LR, Gavrilovic I, Kaley TJ, Nolan CP *et al.* A Phase II Study Assessing Long-term Response to Ibrutinib Monotherapy in Recurrent or Refractory CNS Lymphoma. *Clin Cancer Res* 2024; 30(18): 4005–4015. doi: 10.1158/1078-0432.CCR-24-0605
40. Braggio E, Van Wier S, Ojha J, McPhail E, Asmann YW, Egan J *et al.*Genome-Wide Analysis Uncovers Novel Recurrent Alterations in Primary Central Nervous System Lymphomas. *Clin Cancer Res* 2015; 21(17): 3986–3994. e-pub ahead of print 20150519; doi: 10.1158/1078-0432.CCR-14-2116
41. Gonzalez-Aguilar A, Idbaih A, Boisselier B, Habbita N, Rossetto M, Laurenge A *et al.*Recurrent mutations of MYD88 and TBL1XR1 in primary central nervous system lymphomas. *Clin Cancer Res* 2012; 18(19): 5203–5211. e-pub ahead of print 20120726; doi: 10.1158/1078-0432.CCR-12-0845

Table 2

Table 2 is available in the Supplementary Files section.

Figures

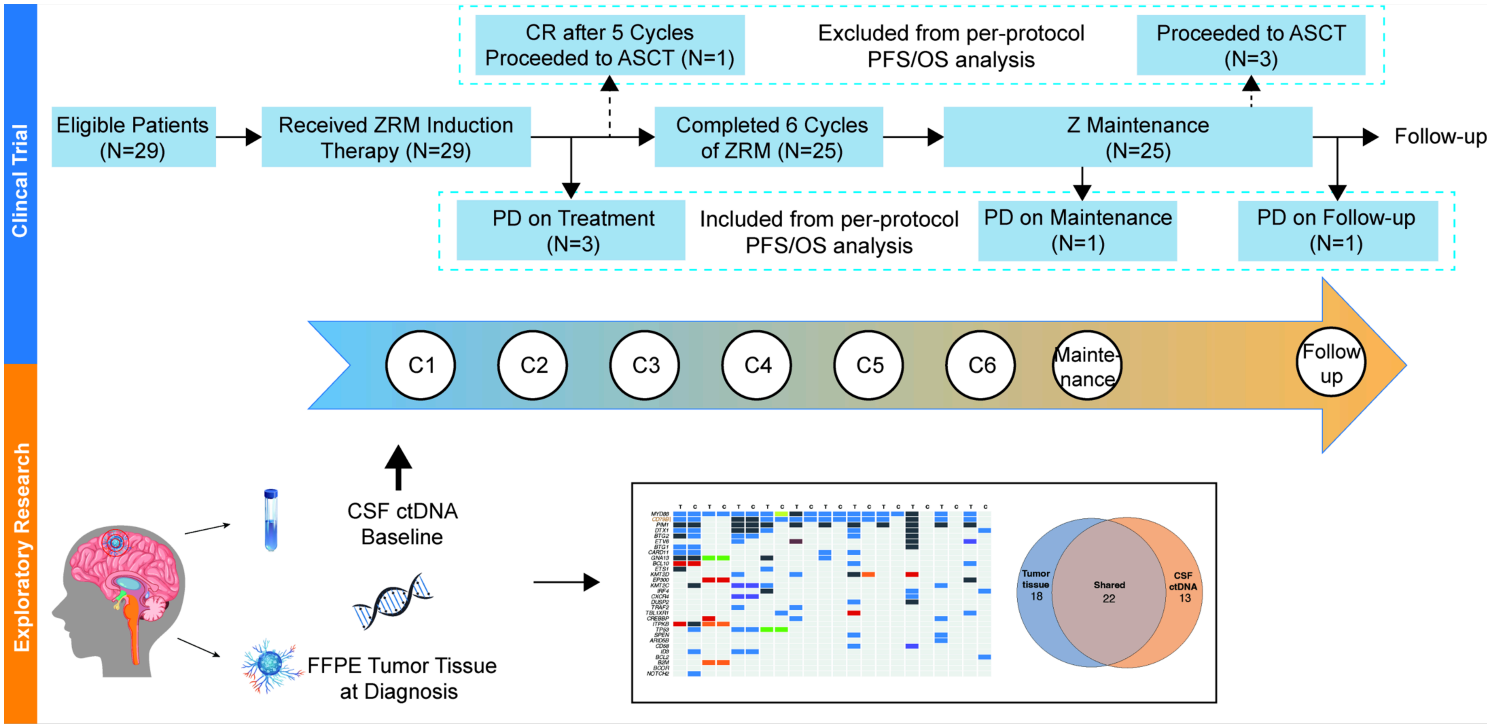

Figure 1

Study design and sample collection workflow.

A total of 29 eligible patients with newly diagnosed PCNSL received zanubrutinib–rituximab–methotrexate (ZRM) induction therapy. Patients received up to six cycles of ZRM induction followed by zanubrutinib maintenance when applicable. Four patients proceeded to autologous stem-cell transplantation (ASCT) after achieving remission and were excluded from the per-protocol PFS/OS

analysis but retained in baseline, response, safety, and descriptive treatment-course analyses. CSF samples were collected at baseline and during treatment for ctDNA profiling. Formalin-fixed, paraffin-embedded tumor tissue was used for genomic profiling when available.

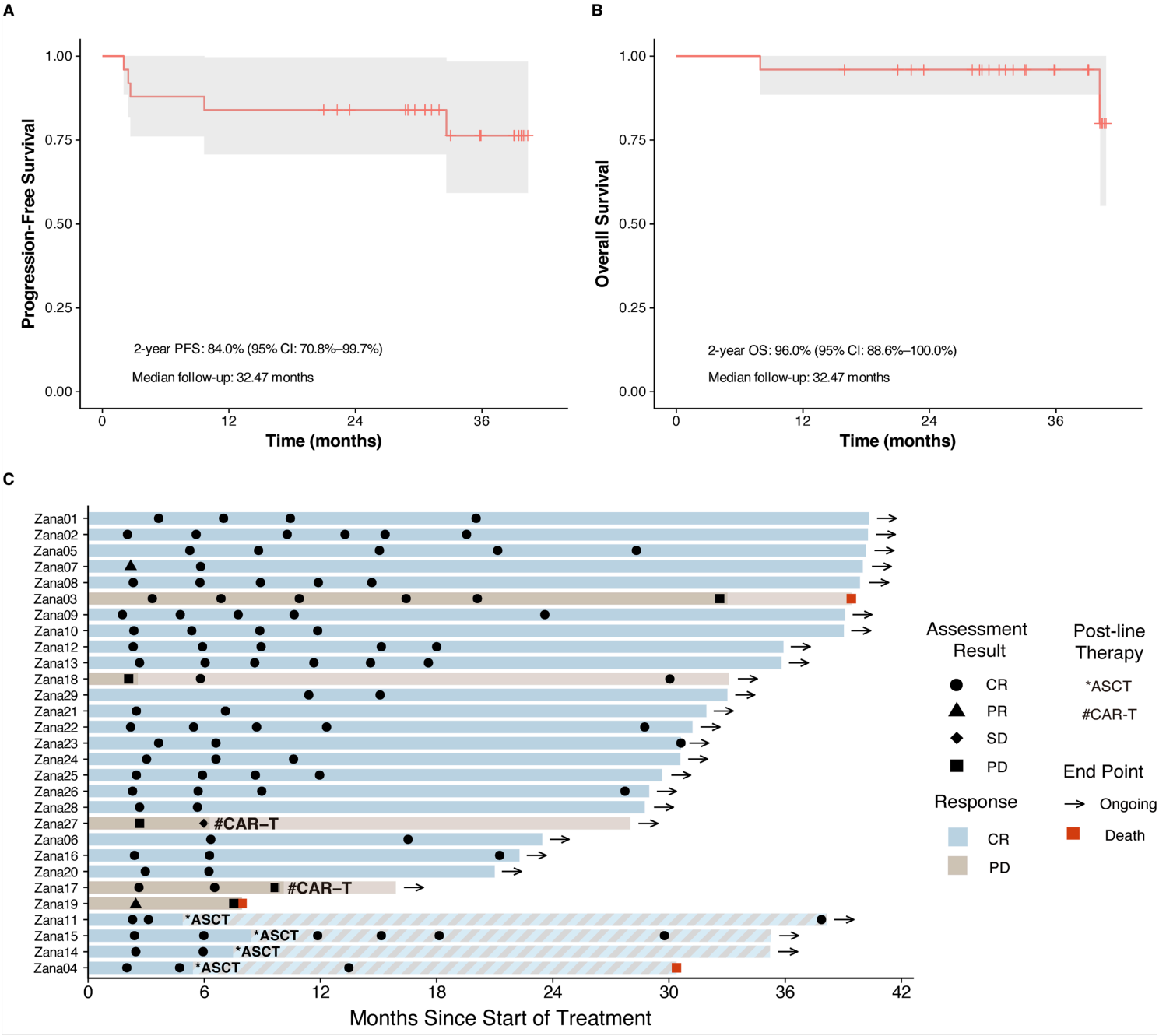

Figure 2

Clinical outcomes and individual treatment courses.

(A) Kaplan–Meier curve of progression-free survival (PFS) in the per-protocol cohort excluding patients who underwent ASCT after remission (n = 25). The estimated 2-year PFS was 84.0% (95% CI, 70.8–99.7).

(B) Kaplan–Meier curve of overall survival (OS) in the per-protocol cohort (n = 25). The estimated 2-year OS was 96.0% (95% CI, 88.6–100). Shaded areas represent 95% confidence intervals.

(C) Swimmer plot showing individual treatment duration, serial response assessments, end-of-treatment (EOT) response, and subsequent therapies in all enrolled patients (n = 29). EOT response was defined as the last response assessment during first-line protocol treatment; for patients who proceeded to post-line treatment such as ASCT or CAR-T, EOT response was defined as the last response assessment before those therapy. Patients who underwent ASCT after remission and patients who subsequently received additional CAR-T are indicated.

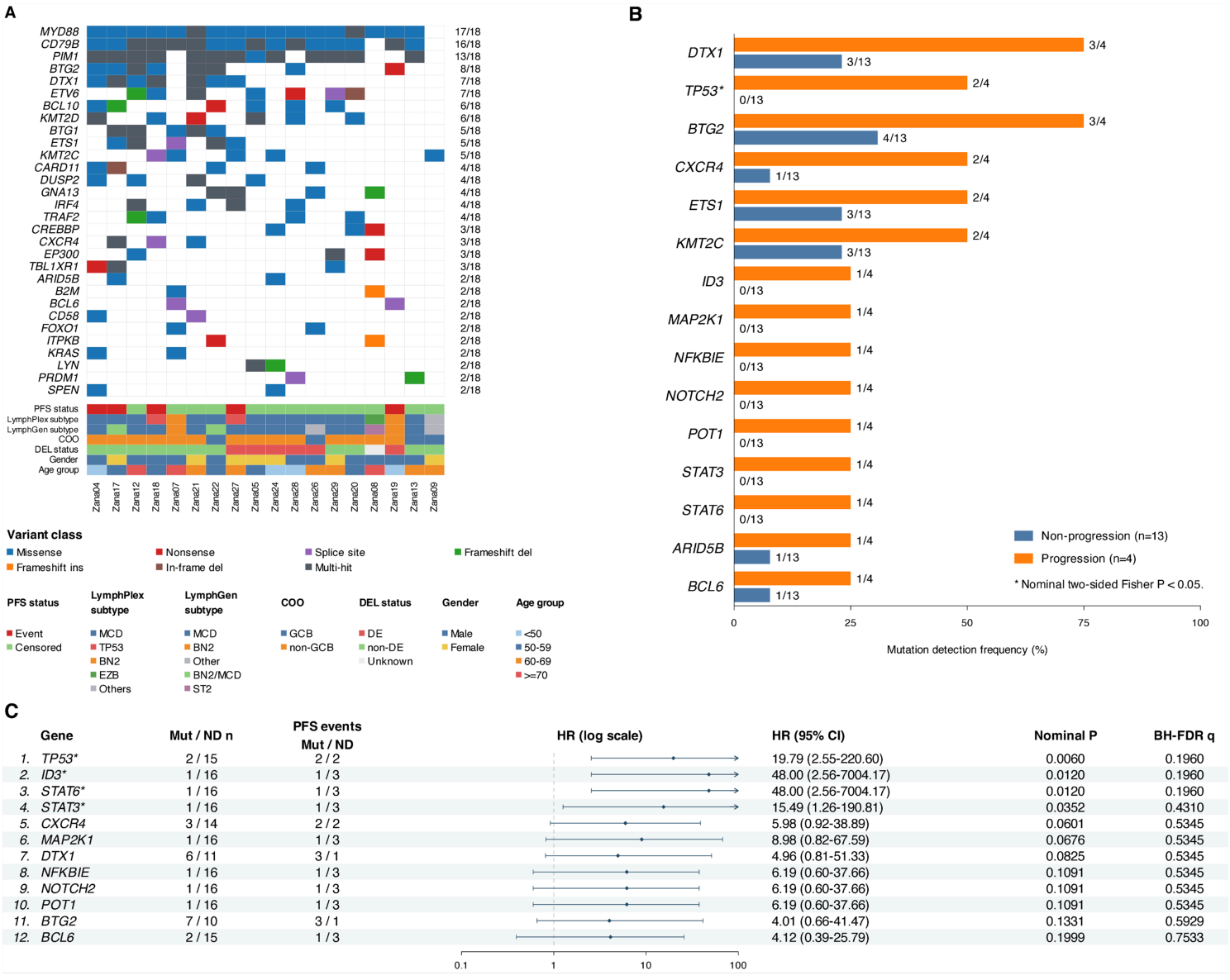

C

	Gene	Mut / ND n	PFS events Mut / ND	HR (log scale)	HR (95% CI)	Nominal P	BH-FDR q
1.	*TP53**	2 / 15	2 / 2		19.79 (2.55-220.60)	0.0060	0.1960
2.	*ID3**	1 / 16	1 / 3		48.00 (2.56-7004.17)	0.0120	0.1960
3.	*STAT6**	1 / 16	1 / 3		48.00 (2.56-7004.17)	0.0120	0.1960
4.	*STAT3**	1 / 16	1 / 3		15.49 (1.26-190.81)	0.0352	0.4310
5.	*CXCR4*	3 / 14	2 / 2		5.98 (0.92-38.89)	0.0601	0.5345
6.	*MAP2K1*	1 / 16	1 / 3		8.98 (0.82-67.59)	0.0676	0.5345
7.	*DTX1*	6 / 11	3 / 1		4.96 (0.81-51.33)	0.0825	0.5345
8.	*NFKBIE*	1 / 16	1 / 3		6.19 (0.60-37.66)	0.1091	0.5345
9.	*NOTCH2*	1 / 16	1 / 3		6.19 (0.60-37.66)	0.1091	0.5345
10.	*POT1*	1 / 16	1 / 3		6.19 (0.60-37.66)	0.1091	0.5345
11.	*BTG2*	7 / 10	3 / 1		4.01 (0.66-41.47)	0.1331	0.5929
12.	*BCL6*	2 / 15	1 / 3		4.12 (0.39-25.79)	0.1999	0.7533

0.1 1 10 100

Figure 3

Tumor-tissue genomic landscape and tumor-derived candidate alterations associated with PFS.

(A) Oncoplot of top 30 mutated genes in 18 evaluable tumor tissue samples. Variant classes are color-coded as indicated. Bottom annotation tracks summarize clinicopathologic variables, including

progression status, cell-of-origin subtype, double-expression status, gender, age group, and molecular subtype.

(B) Tumor-tissue mutation-frequency comparison between patients with and without subsequent progression. Genes are ranked by mutation-frequency difference between progression and non-progression groups. Fisher's exact test was used for exploratory comparisons. Nominal P values were not adjusted for multiple testing.

(C) Exploratory univariable Cox analysis of PFS by tumor-tissue mutation status. Hazard ratios compare mutation-positive versus mutation-negative patients. Estimates should be interpreted cautiously because of the limited number of evaluable samples and PFS events.

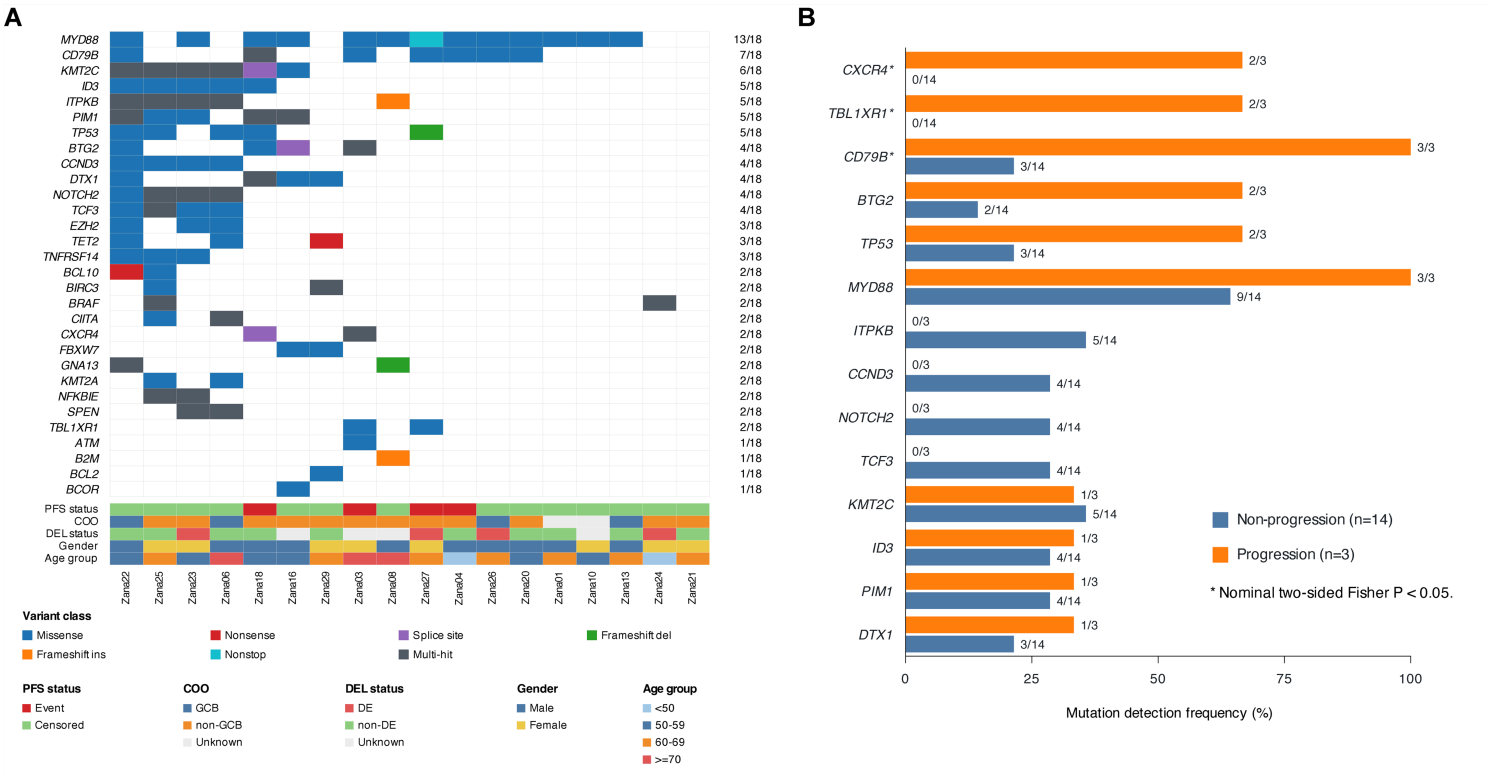

C

Gene	Mut / ND n	PFS events Mut / ND	HR (log scale)	HR (95% CI)	Nominal P	BH-FDR q
*1. CD79B**	6 / 11	3 / 0		21.34 (1.92-2929.44)	0.0103	0.3136
*2. CXCR4**	2 / 15	2 / 1		14.26 (1.77-164.28)	0.0143	0.3136
*3. TBL1XR1**	2 / 15	2 / 1		10.74 (1.41-118.17)	0.0235	0.3447
*4. TP53**	5 / 12	2 / 1		13.51 (1.09-1866.42)	0.0420	0.4618
5. BTG2	4 / 13	2 / 1		6.93 (0.91-76.24)	0.0607	0.5339
6. ATM	1 / 16	1 / 2		6.11 (0.51-50.34)	0.1330	0.9444
7. ID3	5 / 12	1 / 2		2.68 (0.22-33.18)	0.4029	0.9444
8. PIM1	5 / 12	1 / 2		2.68 (0.22-33.18)	0.4029	0.9444
9. DTX1	4 / 13	1 / 2		2.46 (0.22-18.72)	0.4089	0.9444
10. MYD88	12 / 5	3 / 0		2.52 (0.24-341.60)	0.4994	0.9444
11. ITPKB	5 / 12	0 / 3		0.40 (0.00-4.25)	0.4994	0.9444
12. BCOR	1 / 16	0 / 3		3.10 (0.02-38.08)	0.5210	0.9444

0.1 1 10 100

Figure 4

Genomic alterations in baseline CSF ctDNA and their association with clinical outcomes.

(A) Oncoplot of top 30 mutated genes in baseline CSF ctDNA from 18 evaluable patients (out of 21 successfully sequenced cases; 3 excluded due to low VAF or absence of detectable meaningful

mutations). Variant classes are color-coded as indicated. Bottom annotation tracks summarize progression status, cell-of-origin subtype, double-expression status, gender, and age group.

(B) Mutation frequencies stratified by progression status. Genes are ranked by mutation-frequency difference between progression and non-progression groups. Fisher’s exact test was used for exploratory comparisons. Nominal P values were not adjusted for multiple testing..

(C) Univariate Cox regression of PFS by baseline CSF ctDNA mutations. Hazard ratios compare mutation-positive versus mutation-negative patients. Only genes meeting prespecified mutation-frequency and model-stability criteria are displayed. Estimates should be interpreted cautiously because of the limited number of PFS events.

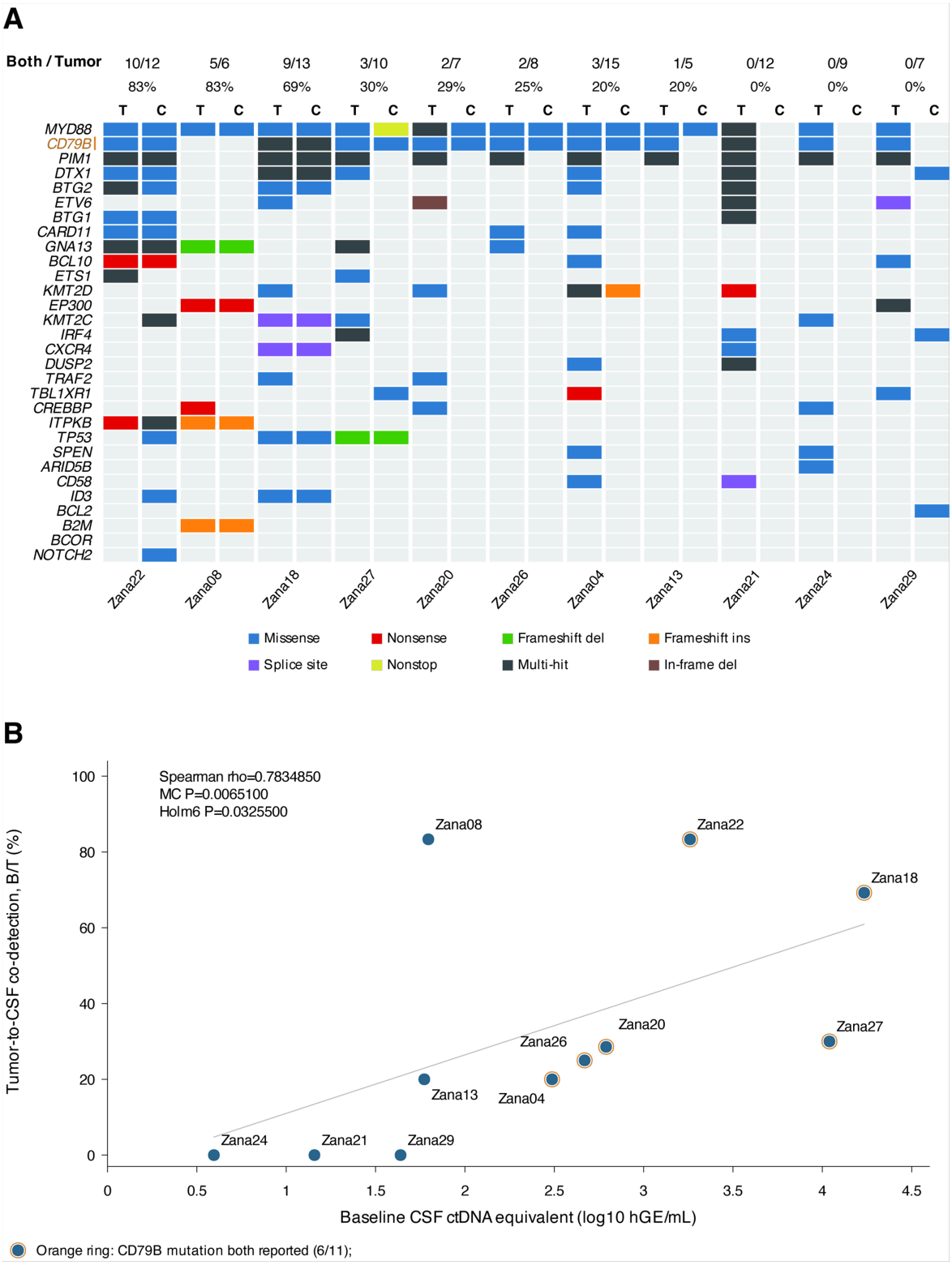

Figure 5

Paired tumor tissue and CSF ctDNA mutational profiles and their association with baseline CSF ctDNA abundance.

(A) Paired oncoplot showing mutation profiles in diagnostic tumor tissue (T) and matched baseline cerebrospinal fluid (CSF) ctDNA (C) from 11 patients. Each patient is represented by two adjacent

columns, with tumor tissue on the left and CSF ctDNA on the right. The oncoplot displays 30 selected genes, while gene-level co-detection was assessed across the 86 genes of the panel. The numbers above each patient indicate the proportion of tumor-reported genes also detected in matched CSF (Both/Tumor). Across all 11 pairs, 35 of 104 tumor-reported patient–gene observations (33.7%) were also detected in CSF, with a median patient-level co-detection fraction of 25.0%.

(B) Association between baseline CSF ctDNA abundance (log10 hGE/mL) and the patient-level proportion of tumor-reported genes also detected in CSF. Each point represents one patient (n=11). A positive correlation was observed. The line illustrates the overall trend. Gene-level co-detection does not necessarily indicate identical variants in the two specimen types.

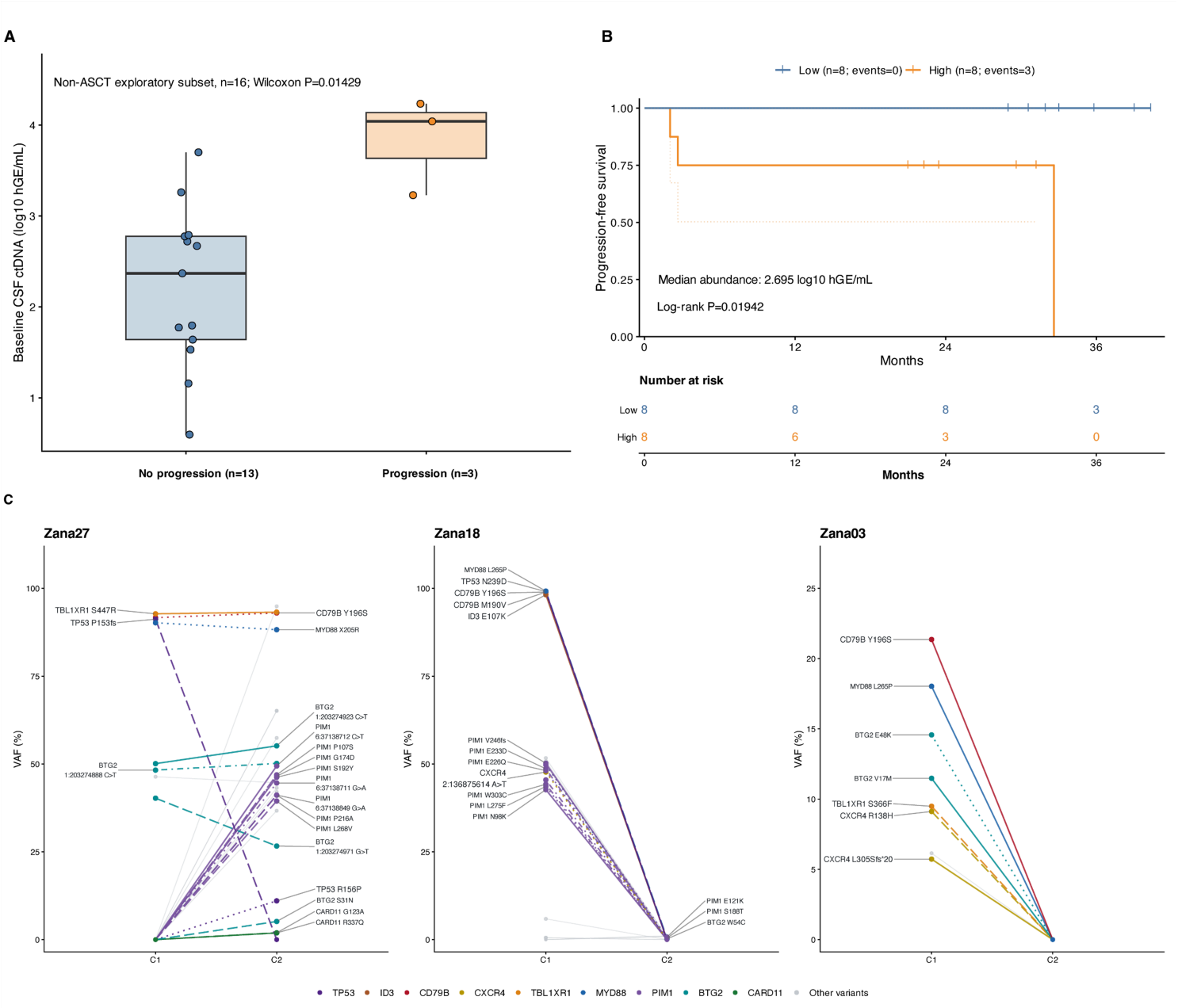

Figure 6

Baseline CSF ctDNA burden and progression risk.

(A) Baseline CSF ctDNA burden stratified by subsequent progression status. The Wilcoxon rank-sum test was used for comparison.

(B) Kaplan–Meier analysis of PFS stratified by median baseline CSF ctDNA burden. The log-rank test was used for comparison. The number-at-risk table is shown below the plot.

(C) Serial variant allele frequency trajectories of selected CSF ctDNA mutations in representative patients who experienced progression. Each line represents a distinct mutation.

Supplementary Files

This is a list of supplementary files associated with this preprint. Click to download.

- Table2AE.xlsx
- suppFig2.tif
- suppFig1.tif
- SuppTable1Cox.pdf